

Application of the Finite Element Method In Cold Forging Processes

Cristina Maria Oliveira Lima Roque

Sérgio Tonini Button

Universidade Estadual de Campinas, Faculdade de Engenharia Mecânica, Departamento de Engenharia de Materiais, 13080-970 – Campinas – SP
sergio1@fem.unicamp.br

The demand for more efficient manufacturing processes has been increasing in the last few years. The cold forging process is presented as a possible solution, because it allows the production of parts with a good surface finish and with good mechanical properties. Nevertheless, the cold forming sequence design is very empirical and it is based on the designer experience. The computational modeling of each forming process stage by the finite element method can make the sequence design faster and more efficient, decreasing the use of conventional “trial and error” methods. In this study, the application of a commercial general finite element software - ANSYS - has been applied to model a forming operation. Models have been developed to simulate the ring compression test and to simulate a basic forming operation (upsetting) that is applied in most of the cold forging parts sequences. The simulated upsetting operation is one stage of the automotive starter parts manufacturing process. Experiments have been done to obtain the stress-strain material curve, the material flow during the simulated stage, and the required forming force. These experiments provided results used as numerical model input data and as validation of model results. The comparison between experiments and numerical results confirms the developed methodology potential on die filling prediction.

Keyword: Metal forming, finite element analysis, Ansys, elasto-plasticity, cold forging design.

Introduction

Metal forming is a widely used manufacturing process noted for its minimum waste and dimensional precision, and it usually improves the mechanical properties of the formed part. However, the forming sequence of a new design is not a straightforward task, and it requires many trials and adjustments to achieve satisfactory producing conditions. The empirical “trial and error” method has been traditionally applied to metal forming design, however, this approach is expensive and time consuming.

Computer simulation has become reliable and acceptable in the metal forming industry since the 1980's. Metal forming analysis can be performed in three modeling scales (Koop et al., 1997). The first scale is the global modeling, which only predicts process loads or work. Analytical methods are used for this purpose. Local scale analysis is used to estimate the thermo-mechanical variables such as strain, strain rate, and temperature.

With the extensive development in computational mechanics, numerical methods have been used as an economical alternative to perform the local modeling. Micro-scale modeling computes the micro-structural evolution during the forming process. Since global scale analysis is only applicable to simple situations and micro modeling is still incipient and only gives results for specific conditions, local modeling is the most popular approach. Among other methods, the Finite Element Methods (FEM) is widely used in metal forming analysis due to its capabilities to model the complicated geometries of tools and parts in forming processes.

In this paper, we present two forming problems. Ring compression test and upsetting simulations are presented to demonstrate the capabilities of a finite element commercial software (Ansys) to aid in metal forming design. The contact conditions are modeled by the Coulomb law with a penalty method and the multilinear elasto-plastic material model is used. Experiments are carried out to validate the modeling technique.

3/4 3/4 Nomenclature 3/4

C^s - elastic tangent operator
 E - Young's modulus
 F_n - normal contact force

G - prescribed displacement
 h - surface traction
hf - final height

e^p - plastic strain rate
 λ - plasticity consistency parameter

F_t - tangential contact force	ho - initial height	μ - friction coefficient
K - stiffness matrix	n - normal vector of $\Gamma_x^{h_i}$	\mathbf{S} - yield stress
S - deviatoric Cauchy stress	t_n - normal contact traction	Ω - n-dimensional domain
X - position vector in the undeformed state	t_t - tangential contact traction	Γ - boundary of Ω
b - body force	u - displacement	Γ^c - part of the boundary where the contact tractions are present
d - displacement vector	v - velocity	Γ_x^e - part of the boundary where natural conditions are prescribed
dif - final internal diameter	x - position vector in the deformed state	Γ_x^e - part of the boundary where essential conditions are prescribed
dio - initial internal diameter	a - back stress	
e^p - effective plastic strain	a_t, a_n - penalty numbers	
f - force vector	e - strain rate	

Cold Forging Processes

One of the biggest challenges in the metal forming industry is to obtain products in the final shape and properties with minimum machining. Cold forging processes are a viable option for this purpose because the manufactured part needs little machining, small production time, and the products present mechanical strength higher than parts manufactured by other processes.

Cold forging is a process carried out below the recrystallization temperature applied to manufacture small parts with varied geometries and has the following advantages: minimum material waste, mechanical properties improvement, such as yield strength and hardness, which brings as an advantage the use of cheaper materials, very good surface finish, energy economy when compared with hot or warm forging, and tools subjected to less thermal fatigue.

Finite Element Formulation In Elasto-Plasticity with Contact Condition

Considering a fixed Cartesian coordinate system in a domain Ω , and denoting the nodal positions in the initial configuration Ω_x by X and those in the deformed configuration Ω_x by a mapping function φ where $x = \varphi(X, t)$, the problem statement can be defined as follows: given body force $b_i(x)$, surface traction $h_i(x)$ on the boundary $\Gamma_x^{h_i}$, boundary displacement $g_i(x)$ on the boundary $\Gamma_x^{g_i}$, initial displacement $u_i^0(X)$, and initial velocity $v_i^0(X)$, find $u_i(x)$ such that they satisfy the following equation:

$$\tau_{ij,j} + b_i = 0 \quad \text{in } \Omega_x \quad (1)$$

with boundary conditions

$$t_{ij} n_j = h_i \quad \text{on } \Gamma_x^{h_i} \quad (2)$$

$$u_i = g_i \quad \text{on } \Gamma_x^{g_i} \quad (3)$$

and initial conditions

$$u_i(\mathbf{X}, 0) = u_i^0(\mathbf{X}) \quad (4)$$

$$\dot{u}_i(\mathbf{X}, 0) = v_i^0(\mathbf{X}) \quad (5)$$

where the Cauchy stress obtained from the constitutive equations of plasticity are summarized in table 1 [Bathe, 1996a]:

Table 1. Constitutive equations of plasticity.

Stress-strain relation	$\mathbf{t} = \mathbf{C}^e (\dot{\mathbf{e}} - \dot{\mathbf{e}}^P), \quad \varepsilon_{ij} = \frac{1}{2} \left(\frac{\partial u_i}{\partial x_j} + \frac{\partial u_j}{\partial x_i} \right)$
Yield function	$f(\mathbf{x}, K) = \ \mathbf{x}\ - \sqrt{\frac{2}{3}} K (\bar{e}^P), \quad \mathbf{x} = \mathbf{S} - \mathbf{a}$
Flow and hardening rules	$\dot{\mathbf{e}}^P = \dot{\lambda} \frac{\mathbf{x}}{f}, \quad \dot{\mathbf{a}} = \frac{2}{3} H (\bar{e}^P) \dot{\mathbf{e}}^P \quad \text{and} \quad K = K(\bar{e}^P)$
Kuhn-Tucker conditions	$\dot{\lambda} \geq 0, \quad f \leq 0, \quad \dot{\lambda} f = 0$

where \mathbf{S} is the deviatoric Cauchy stress, \mathbf{a} is the back stress, $\dot{\mathbf{e}}$ is the strain rate, $\dot{\mathbf{e}}^P$ is the plastic strain rate, \bar{e}^P is the effective plastic strain, \mathbf{C}^e is the elastic tangent operator, H and K are parameters related to the hardening rule, and λ is the plasticity consistency parameter.

Contact conditions are included to handle contact between tools and dies. The classical Coulomb law [Mielnik, 1991] is used to model frictional contact and the penalty method [Bathe, 1996b] is applied to avoid penetration. The contact tractions on Γ_c are defined as follows:

$$t_n = -\alpha_n g_n$$

$$t_t = \begin{cases} -\alpha_t g_t & \text{if } |\alpha_t g_t| \leq |\mathbf{m}_f t_n| \quad (\text{stick conditions}) \\ -\mathbf{m}_f t_n \operatorname{sgn}(g_t) & \text{otherwise} \quad (\text{slip conditions}) \end{cases} \quad (6)$$

where α_n and α_t are the normal and tangential penalty numbers and g_n and g_t are normal and tangential gaps between contact surfaces.

Using Hill's weak formulation, the variational equation of the problem can be written as

$$\int_{\Omega_x} \mathbf{d}u_{i,j} \mathbf{t}_{ij} d\Omega - \int_{\Omega_x} \mathbf{d}u_i b_i d\Omega - \int_{\Gamma_x^{h_i}} \mathbf{d}u_i h_i d\Gamma + \int_{\Gamma_x^c} (t_n \mathbf{d}g_n + t_t \mathbf{d}g_t) d\Gamma = 0 \quad (7)$$

The contact term is integrated by co-localational formulation to yield

$$\int_{\Gamma_x^c} (t_n \mathbf{d}g_n + t_t \mathbf{d}g_t) d\Gamma = \sum_A (F_n \mathbf{d}g_n + F_t \mathbf{d}g_t)_A \quad (8)$$

where F_n and F_t are the nodal normal and tangential contact forces and A is summed over the contact nodes on the deformable body.

Finite Element Metal Forming Analysis

The elasto-plastic constitutive equation together with contact conditions are used for metal forming analysis. The radial return mapping algorithm is used to compute the stress and internal variables (Krieg and Key, 1976), and the consistent tangent operator (Simo and Taylor, 1985), which preserves the quadratic convergence rate of the Newton method is also used.

The penalty method is applied to impose contact conditions between the contacting surfaces. The friction is an important factor in forming processes, and it is also responsible for the internal and surface quality of the formed part. In the current formulation friction is modeled by the Coulomb law.

Figure 1 shows how a finite element analysis (FEA) can be used in metal forming design. The FEA can provide detailed information for forming designers such as forming force, defects predictions, flow pattern, and stress concentration in the dies. The strain output, for instance, can display strain concentration areas to identify the possible early failures in the tools or to predict formability problems. Therefore, part fabrication design can be modified to improve tool's life or to

enhance the formability conditions, and the new designs can be checked with repeated finite element simulations before experimental tests.

Many forming aspects can be analyzed from simulated solution. For instance, irregular flow, which can cause products internal defects, can be detected from simulation. Die filling problems can also be predicted by deformation pattern and stress/strain solutions. Elastic deformation of the tools, which should be controlled to maintain desirable tolerances, can be verified in the finite element analysis prediction.

The solution convergence of the method is checked by decreasing the time step, and by increasing the number of nodes of the analysis model.

Numerical Examples

Ring Compression

The ring compression test was developed to experimentally estimate the friction coefficient in metal forming operations (Male and Cockcroft, 1965). The test consists of compressing a ring at different ratios with flat and smooth tools and measuring the final height (hf) and final internal diameter (dif). During compression, the internal and external diameters will change according to the amount of compression and the friction condition on the interface. Hence, curves relating changes in the internal diameter with respect to the compression ratio characterize the friction coefficient (μ).

The ring test was simulated with physical properties of the cold forging steel DIN 16MnCr5, considered as multilinear elasto-plastic with yield stress $\bar{\sigma} = 100\text{MPa}$, Young's modulus $E = 208\text{ GPa}$, and Poisson's ratio $\nu = 0.3$. The geometrical dimensions of the ring deo: dio : ho (initial external diameter : initial internal diameter : initial height) are in proportion to 6:3:2. The lubricant used in this test is the bisulfide of molybdenum (MoS₂), which is widely used in cold metal forming processes.

Due to the axial and radial symmetries, the simulation was made with one quarter of the ring (discretized with 231 nodes). Two types of elements were used to model the ring: Visco106 and Plane42 (Ansys - V.III, 1993). Contact was modeled with Contact48 element. In Fig. 2, one quarter of the cross section of the initial ring model is shown. The number of solution time steps was 1000. The prescribed displacement was applied at the flat tool's nodal points.

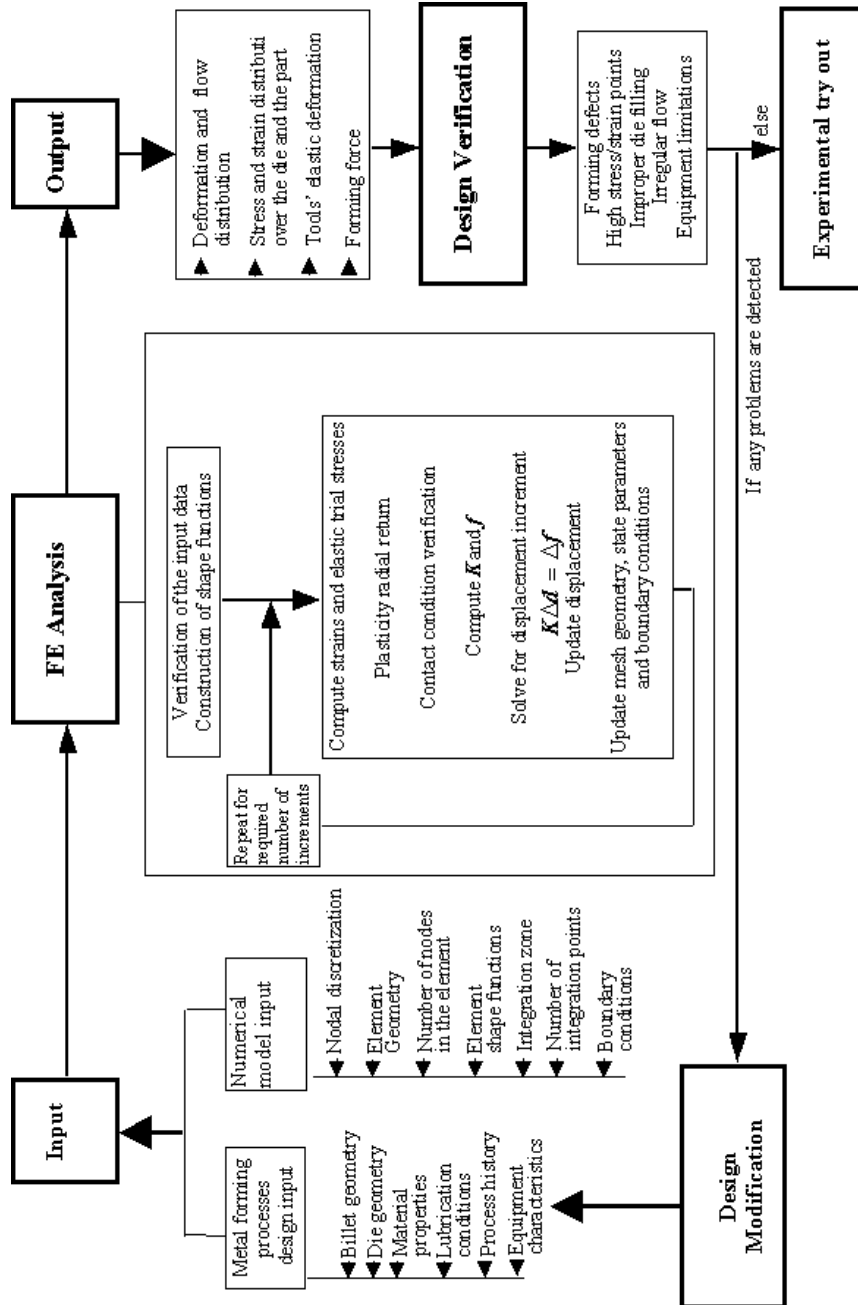


FIGURE 1. Flow chart showing the use of the finite element analysis in a forging problem.

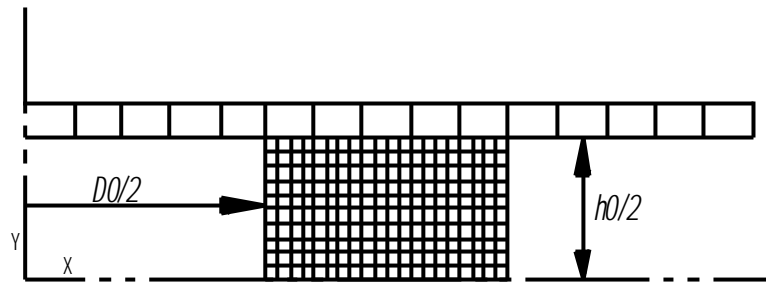


Figure 2. Initial configuration of the ring compression model.

The ring test was simulated with four different friction conditions: $\mu=0$; $\mu=0.15$; $\mu=0.3$; and $\mu=0.57$. The calibration curves obtained by FEM are compared to analytical-empirical results (Male and Cockcroft, 1965) in Fig. 3. The initial (dashed lines) and deformed (straight lines) ring profile are shown for each friction condition in Fig. 4.

The results of the zero friction simulation are close to Male's results (Fig. 3a). In this situation the ring is supposed to deform in a parallel configuration (without barreling). The deformed ring profile obtained by the computational model accurately represents the zero friction situation (Fig. 4a).

The ring test simulation results for friction coefficients $\mu = 0.15$ and $\mu = 0.3$ shown in Fig. 3 (b, c) are in agreement with Male's results (Male and Cockcroft, 1965). Ring profiles (Fig. 4 (b, c)) are consistent with previous results (Kobayashi, 1989).

In the case of maximum friction, or stick condition, the results are not very close to Male's (Fig. 3 (d)), which indicates that barreling effect is not correctly modeled for high friction values

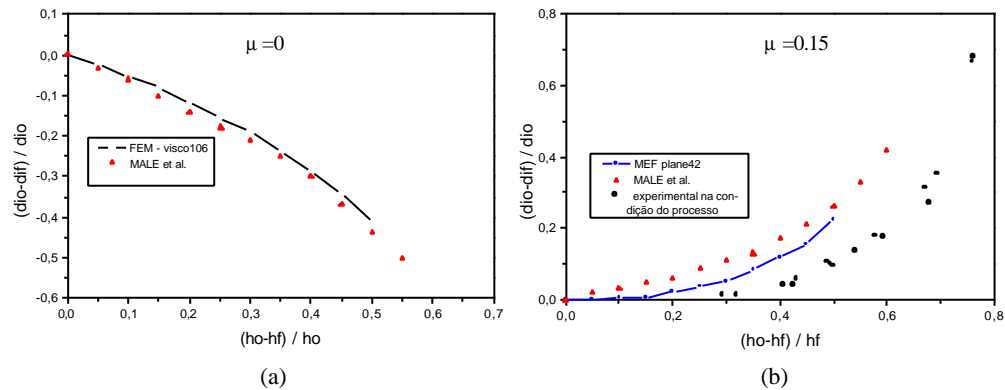


Figure 3. Ring test calibration curves for the following friction conditions: (a) $m=0$; (b) $m=0.15$; (c) $m=0.3$; and (d) stick.

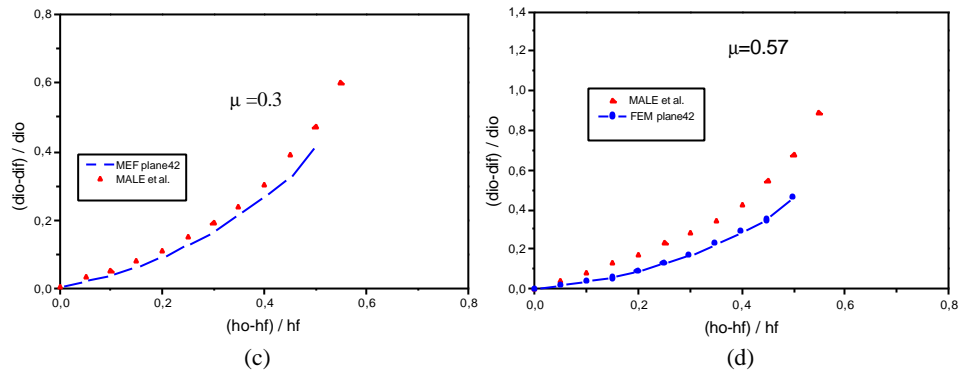
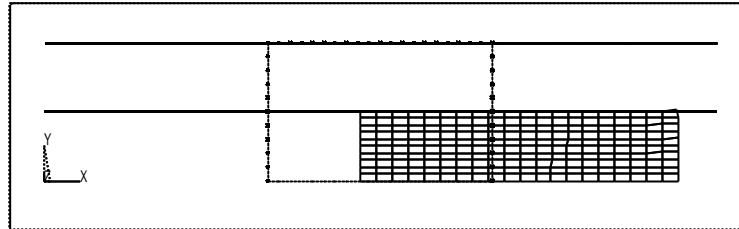


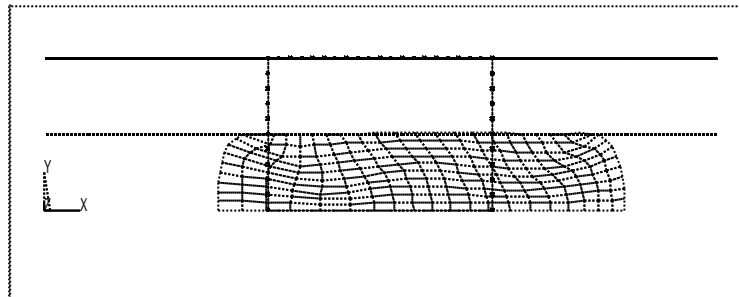
Figure 3. (continued).

In the Fig. 5, Male's calibration curves are presented and in Fig. 6, the calibration curves obtained by numerical method are presented. Comparing the Figs. 5 and 6, we notice that the model has a better prediction for lower friction coefficients and is less sensitive for higher friction coefficients.

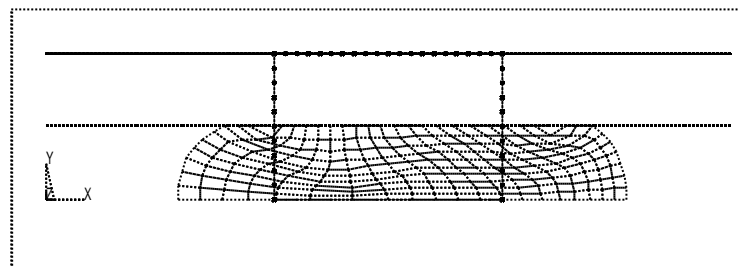
Experimental tests for the lubricated ring were developed [Roque, 1996] and the results were plotted in Figs. 3 (b), 5 and 6 to better estimate the friction coefficient of the upsetting process according to the numerical calibration curves.



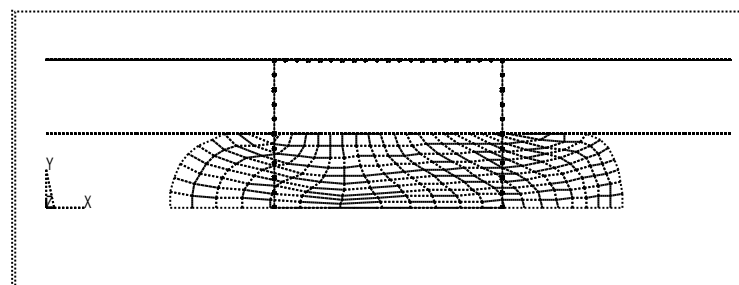
(a)



(b)



(c)



(d)

Figure 4. Deformed ring profile for the following friction conditions:
(a) $m=0$; (b) $m=0.15$; (c) $m=0.3$; and (d) stick condition.

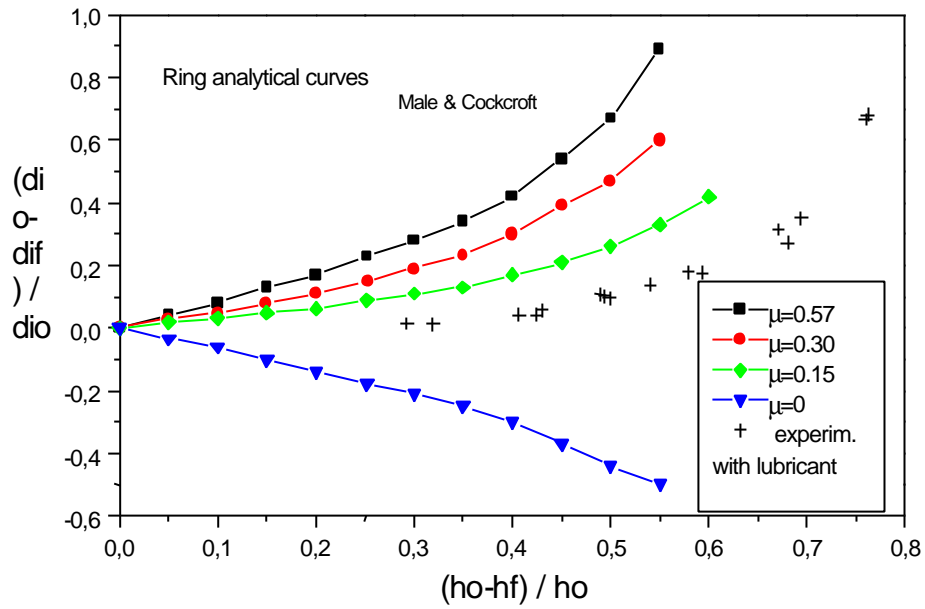


Figure 5. Empirical-analytical ring calibration curves (Male & Cockcroft, 1965).

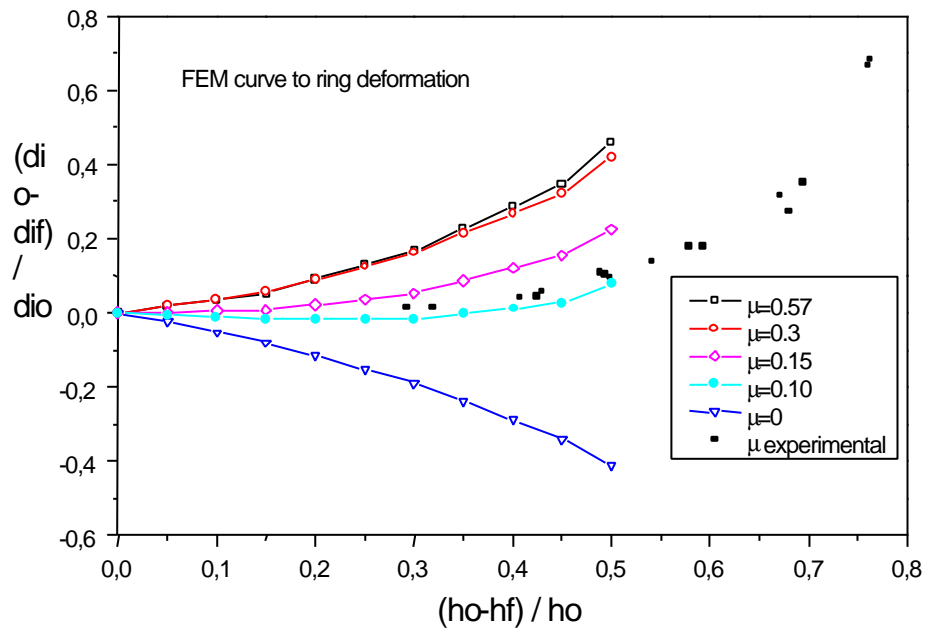


Figure 6. Numerical ring calibration curves.

The friction coefficient for the process was estimated, according to Fig. 6, to be equal to 0.10 for simulation purposes with MoS₂ as lubricant.

Upsetting Problem

The upsetting process of the cold forging steel DIN 16MnCr5 was modeled as shown in Fig. 7. Tools were modeled with Plane42 element and part was modeled with Visco106 element. In this analysis, axisymmetric formulation was used, and prescribed displacement was applied to the punch. The material constants are the following: Young's modulus $E = 208000$ MPa, Poisson's ratio $\nu = 0.3$ and the material was modeled as multilinear elasto-plastic with yield stress $\bar{\sigma} = 100$ MPa in order to consider the work hardening. Coulomb friction (μ) between punch and part is estimated from experiments and simulations of the ring problem, mainly based on the lubrication conditions and tools' finishing surface, and is adopted in the model to be equal to 0.10. The final shape is compared to experimental results (Roque, 1996) in Fig. 8.

The equivalent plastic stress field (Fig. 9) obtained from simulation can be compared to the macro etching section presented in Fig. 10. The darker regions correspond to the most stressed regions. It is possible to detect on the simulated results (Fig. 9) the same arc seen on etched section (Fig. 10) splitting superior (most stressed) from inferior (less stressed) region.

In Fig. 11, some steps of the upsetting operation are presented and it is possible to verify the filling sequence in the die. We can also compare the final deformed grid with the flow lines shown in the macro etching section (Fig. 10).

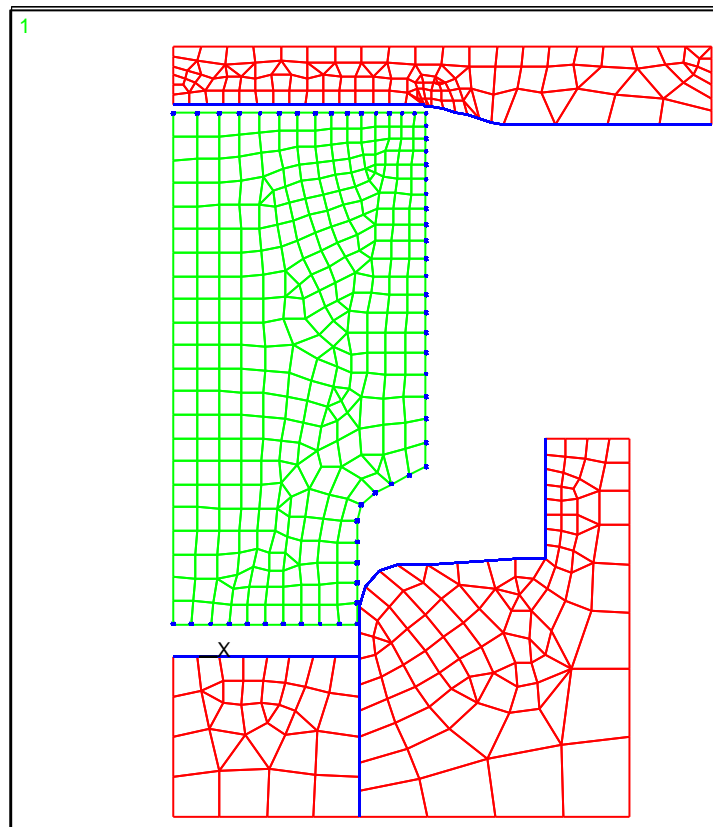


Figure 7 -(a) Discretization of the forging-upsetting operation.

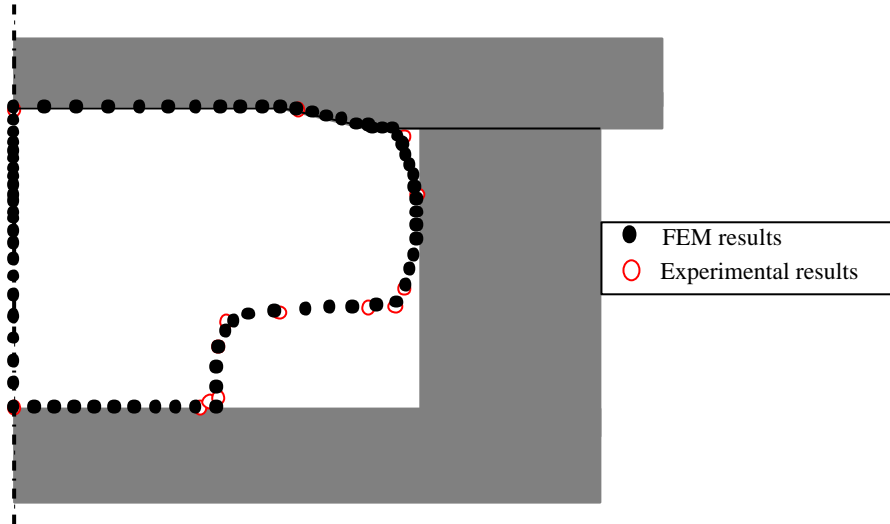


Figure 8. Comparison between real and simulated geometry.

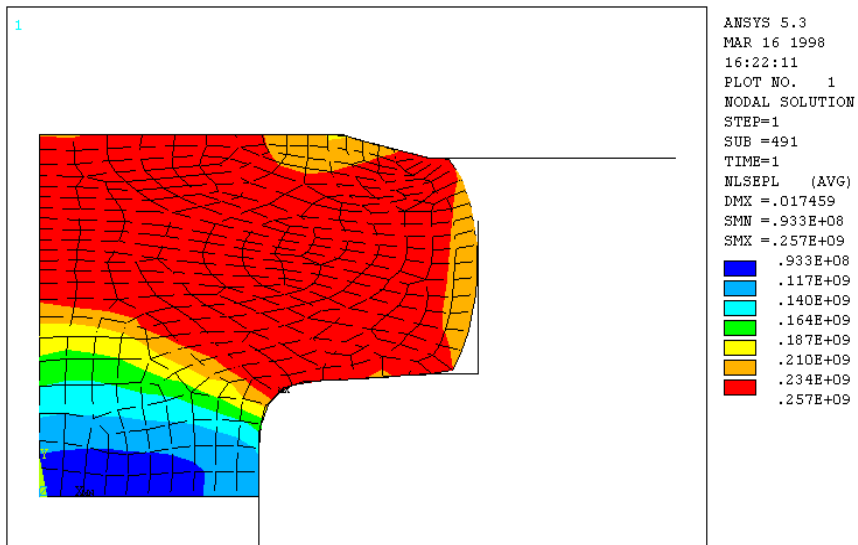


Figure 9. Equivalent plastic stress field.

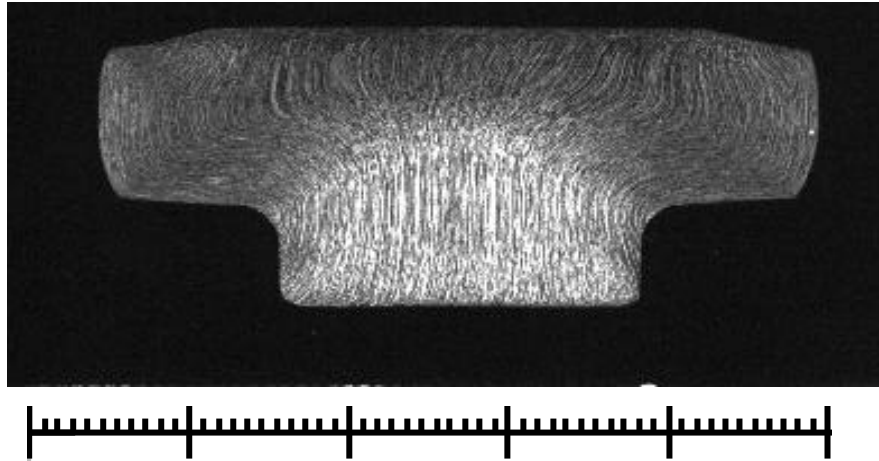


Figure 10. Macro etching showing the flow lines of the formed part.

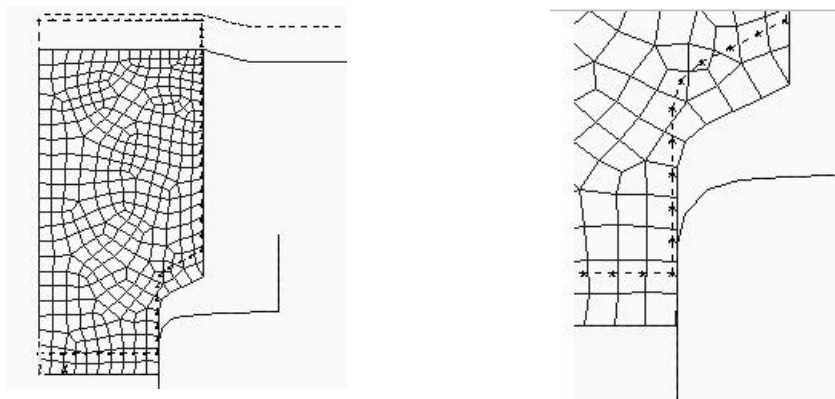


Figure11 – Progressive deformation of the upsetting process.

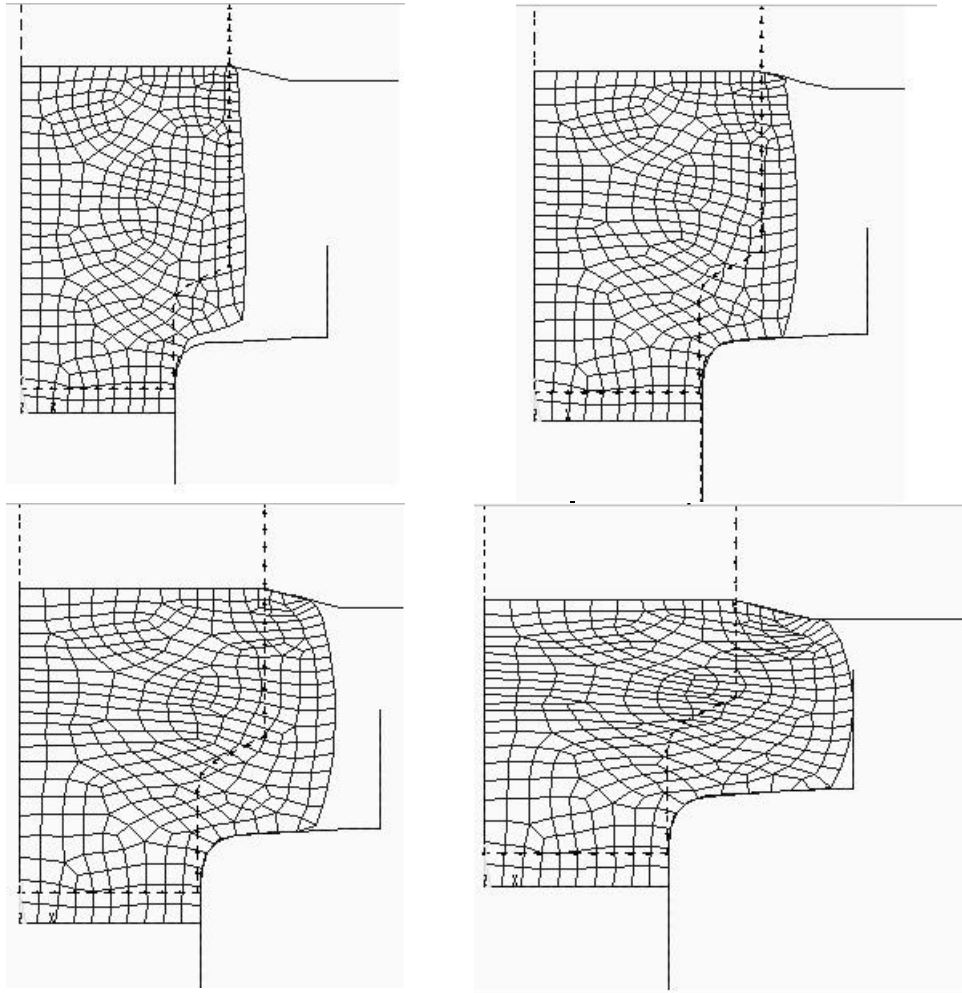


Figure11 – (continued).

Conclusions

Two finite element models were presented: ring test and upsetting. The ring test was modeled and ring experiments were done to estimate the friction coefficient in the upsetting operation according to the numerical calibration curves.

In this analysis, upsetting operation is successfully simulated by the finite element method using the following elements:

Plane42, Visco106, and Contact48. Numerical prediction of the final shape is in good agreement with the experimental

results [Roque, 1996]. Flow stress was predicted properly and the stress field is in accordance with the macro etching. The method was able to predict filling sequence.

Acknowledgments

The Brazilian funding agency Capes – Fundação Coordenação de Aperfeiçoamento de Pessoal de Nível Superior, and Robert Bosch do Brasil are greatly acknowledged for the fellowship given to the first author.

References

- ALTAN, T., 1983, "Metal Forming: fundamentals and applications", ASM, Metals Park, OH.
- ANSYS user's manual for rev. 5.0, 1993, v. III - Elements Manual.
- BATHE, K.-J., 1996a, "Finite Element Procedures", Prentice-Hall, p. 597.
- BATHE, K.-J., 1996b, "Finite Element Procedures", Prentice-Hall, p. 622.
- KRIEG, R.D.; KEY, S.W., 1976, "Implementation of a Time-Independent Plasticity Theory into Structural Computer Programs" in "Constitutive Equations in Viscoplasticity: Computational and Engineering Aspects", J.A. Stricklin and K.J. Saczalski (eds.), AMD-20, ASME, NY.
- KOBAYASHI, S.; OH, S.-I.; ALTAN, T., 1989, "Metal Forming and the Finite Element Method", 1st ed., vol. 1. (Series Eds.: Crookall, J.R., Shaw, M.C.) Oxford University Press, Oxford, 377 p.
- KOPP, R.; CAO, M.L.; DE SOUZA, M.M., 1987, "Multi-level Simulation of Metal Forming Process", Proc. 2nd ITCP, Stuttgart, August, p. 1128-1234.
- MALE, A.T.; COCKCROFT, M. G., 1965, "A Method for the Determination of the Coefficient of Friction of Metals under Conditions of Bulk Plastic Deformation", J. Inst. Metals, v. 93, p. 38-46.
- MIELNIK, E.M., "Metalworking Science and Engineering", McGraw Hill, p. 487, 1991.
- ROQUE, C.M.O.L., 1996, "On the Application of the Finite Element Method in the Planning of the Cold Forging Process", Master Dissertation, UNICAMP, Campinas, SP, Brazil.
- SIMO, J.C.; TAYLOR, R.L., 1985, "Consistent Tangent Operators for Rate-Independent Elasto-Plasticity", Comput. Meth. Appl. Mech. Engrg., v. 48, p. 101-118.